# Schwarzschild Metric - Theory, Simulations and Observations

Hanno Rein
http://hanno-rein.de
Cambridge University

December 2, 2006

This is a handout produced for a seminar talk at the University of Cambridge, presented on the 30th of November 2006.

*Hanno Rein - Cambridge, December 2006*
*http://hanno-rein.de*

# 1 Theory

## 1.1 Derivation of the Schwarzschild Metric

We want to derive a spherical symmetric metric. As a starting point we choose the metric to be

$$ds^2 = g_{00}(r,t)c^2dt^2 + g_{rr}(r,t)dr^2 + r^2(d\Theta^2 + \sin^2\Theta d\phi^2). \tag{1}$$

Hence we are looking for two unknown scalar functions, namely $g_{00}$ and $g_{rr}$. For the following calculation we define

$$-e^\nu = g_{00} = (g^{00})^{-1} \quad \text{and} \quad e^\rho = g_{rr} = (g^{rr})^{-1}.$$

To get the unknown functions we have to solve the Einstein Field Equations. Therefore we need the Christoffel Symbols

$$\Gamma^i_{km} = \frac{1}{2}g^{in}(g_{kn,m} + g_{mn,k} - g_{km,n}).$$

Where "$,k$" denotes the partial derivative. In general it is very hard to calculate these symbols, because for each combination of $i,k$ and $m$ we have to calculate 12 derivatives of the metric tensors. But there is another, more efficient way to get them, which we will discuss now.

The Geodesic Equation describes the motion of a particle and is given by

$$\frac{dx^\mu}{d\sigma^2} + \Gamma^\mu_{\nu\lambda}\frac{dx^\nu}{d\sigma}\frac{dx^\mu}{d\sigma} = 0. \tag{2}$$

But the Euler-Lagrange Equation

$$\frac{d}{d\sigma}\frac{\partial L}{\partial \dot{x}^\mu} - \frac{\partial L}{\partial x^\mu} = 0 \tag{3}$$

does the same. We choose the Lagrangian $L$ to be

$$L = \frac{1}{2}g_{\mu\nu}\frac{dx^\mu}{d\sigma}\frac{dx^\nu}{d\sigma} \tag{4}$$

$$= \frac{1}{2}\left[-e^\nu\left(\frac{dx^0}{d\sigma}\right)^2 + e^\rho\left(\frac{dr}{d\sigma}\right)^2 + r^2\left(\frac{d\Theta}{d\sigma}\right)^2 + r^2\sin^2\Theta\left(\frac{d\phi}{d\sigma}\right)^2\right] \tag{5}$$

The idea is to compare the Geodesic Equation (2) and the Euler-Lagrange Equation (3) to read of the Christoffel Symbols $\Gamma^i_{km}$. We'll do this just for $\mu = 0$ in the Euler Lagrange Equation, but the calculation is very similar in the other cases. This turns out to be

$$\frac{\partial L}{\partial x^0} = \frac{1}{2}\left[-\dot{\nu}e^\nu\left(\frac{dx^0}{d\sigma}\right)^2 + \dot{\rho}e^\rho\left(\frac{dr}{d\sigma}\right)^2\right] \tag{6}$$

$$\frac{\partial L}{\partial \dot{x}^0} = -e^\nu\frac{dx^0}{d\sigma}. \tag{7}$$

And hence we get

$$0 = -e^\nu\left[\frac{d^2x^0}{d\sigma^2} + \underbrace{\nu'}_{=2\Gamma^0_{r0}}\frac{dr}{d\sigma}\frac{dx^0}{d\sigma} - \underbrace{\frac{1}{2}\dot{\nu}}_{=\Gamma^0_{00}}\left(\frac{dx^0}{d\sigma}\right)^2 + \underbrace{\frac{1}{2}\dot{\rho}e^{\rho-\nu}}_{\Gamma^0_{rr}}\left(\frac{dr}{d\sigma}\right)^2\right]. \tag{8}$$

Now we can calculate the components of the Ricci tensor

$$R_{00} = -\left(\frac{\nu''}{2} + \frac{\nu'^2}{4} - \frac{\nu'\rho'}{4} + \frac{\nu'}{r}\right)e^{\nu-\mu} + \left(\frac{\ddot{\rho}}{2} + \frac{\dot{\rho}^2}{4} - \frac{\dot{\nu}\dot{\rho}}{4}\right) \tag{9}$$

$$R_{rr} = \left(\frac{\nu''}{2} + \frac{\nu'^2}{4} - \frac{\nu'\rho'}{4} - \frac{\rho'}{r}\right) - \left(\frac{\ddot{\rho}}{2} + \frac{\dot{\rho}^2}{4} - \frac{\dot{\nu}\dot{\rho}}{4}\right)e^{\rho-\nu} \tag{10}$$

$$R_{0r} = -\frac{\dot{\rho}}{r} \tag{11}$$

$$R_{\Theta\Theta} = \left[1 + \frac{r}{2}\left(\nu' - \rho'\right)\right]e^{-\rho} - 1 \tag{12}$$

$$R_{\phi\phi} = \sin^2\Theta \cdot R_{\Theta\Theta} \tag{13}$$

Outside the source the Einstein Field Equations imply

$$R_{\mu\nu} = 0. \tag{14}$$

We only consider static solutions. Hence $\dot{\nu} = \dot{\rho} = \ddot{\rho} = 0$. It turns out that the solution is always static in a spherical symmetric vacuum solution to $R_{\mu\nu} = 0$. This is known as the Birkhoff theorem, see [Che05].
Finally we have to solve

$$0 = R_{00} = \frac{\nu''}{2} + \frac{\nu'^2}{4} - \frac{\nu'\rho'}{4} + \frac{\nu'}{r} \tag{15}$$

$$0 = e^{\rho-\nu}R_{00} + R_{rr} = \nu' + \rho' \tag{16}$$

$$0 = R_{\Theta\Theta} = \left[1 + \frac{r}{2}\left(\nu' - \rho'\right)\right]e^{-\rho} - 1 \tag{17}$$

Note that there are only two independent equations for 2 functions. One equation is redundant, so we will only solve (16) and (17). After integrating over $r$, (16) gives

$$\rho(r) = -\nu(r)$$

$$\Rightarrow -g_{00} = \frac{1}{g_{rr}}$$

We insert this into (17)

$$(1 - r\rho')e^{-\rho} - 1 = 0$$

and define $\lambda(r) = e^{-\rho}$. Hence

$$\lambda' + \frac{1}{r}\lambda = \frac{1}{r}$$

The solution for this equation is

$$\lambda = 1 - \frac{r^\star}{r} = \frac{1}{g_{rr}} = -g_{00}.$$

Where $r^\star$ is a constant. So we have finally derived the Schwarzschild metric

$$g_{\mu\nu} = \begin{pmatrix} -1 + \frac{r^\star}{r} & 0 & 0 & 0 \\ 0 & \left(1 - \frac{r^\star}{r}\right)^{-1} & 0 & 0 \\ 0 & 0 & r^2 & 0 \\ 0 & 0 & 0 & r^2\sin^2\Theta \end{pmatrix} \tag{18}$$

## 1.2    Motion of a test particle

The motion of a test particle is described by the geodesic equation (3). With the metric (18) the Lagrangian is given by

$$
\begin{aligned}
L &= \left(\frac{\mathrm{d}s}{\mathrm{d}\tau}\right)^2 = g_{\mu\nu}\dot{x}^\mu\dot{x}^\nu & (19)\\
&= \left(-1+\frac{r^\star}{r}\right)c^2\dot{t}^2 + \left(1-\frac{r^\star}{r}\right)^{-1}\dot{r}^2 + r^2\dot{\phi}^2 + r^2\dot{\Theta}^2 = -c^2 & (20)
\end{aligned}
$$

In the last line we restricted the motion wlog to the $\Theta = \frac{\pi}{2}$ plane. Because the Lagrangian (20) does not depend on $t$ and $\phi$ the two quantities

$$
\begin{aligned}
\frac{\partial L}{\partial \dot{\phi}} &= 2r^2\dot{\phi} \equiv \lambda \\
\frac{\partial L}{\partial \dot{t}} &= -2\left(1-\frac{r^\star}{r}\right)c^2\dot{t} \equiv -2c^2\eta
\end{aligned}
$$

are conserved. Hence, the Lagrangian (20) can be rewritten in terms of $\lambda$ and $\eta$

$$
-c^2\frac{1}{2}m\left(1-\frac{r^\star}{r}\right) = -c^2\eta^2\frac{m}{2} + \frac{\dot{r}}{2}m + \frac{\lambda^2}{r^2}\frac{1}{8}m\left(1-\frac{r^\star}{r}\right).
$$

We define

$$
\frac{\lambda^2}{4} = \frac{l^2}{m^2} \qquad \frac{\eta^2-1}{2} \equiv \frac{K}{mc^2} \qquad r^\star \equiv \frac{2GM}{c^2}
$$

and get

$$
K = \frac{1}{2}m\dot{r}^2 + \left(1-\frac{r^\star}{r}\right)\frac{l^2}{2mr^2} - \frac{GmM}{r}.
$$

We identify $K$ as the total (Newtonian) energy of the system and write $K$ as a sum of the kinetic and effective potential energy

$$
K = \frac{1}{2}m\dot{r}^2 + m\Phi_{eff}
$$

with

$$
\Phi_{eff} = -\frac{GM}{r} + \frac{l^2}{2m^2r^2} - \frac{r^\star l^2}{2m^2r^3}. \tag{21}
$$

The first term is the well known Newtonian Potential of a pointmass with mass $M$. The second term is just the rotational energy. But the last term is a new, relativistic effect. It is a $r^{-3}$ correction to the Newtonian Potential.

# 2    Simulations and Observations

## 2.1    Newtonian Potential

In the Newtonian Limit we ignore the $r^{-3}$ term in the potential (21). In Figure 1 you can see that there exists a stable orbit. The solutions are circles and ellipses as shown in Figure 2 and 3.
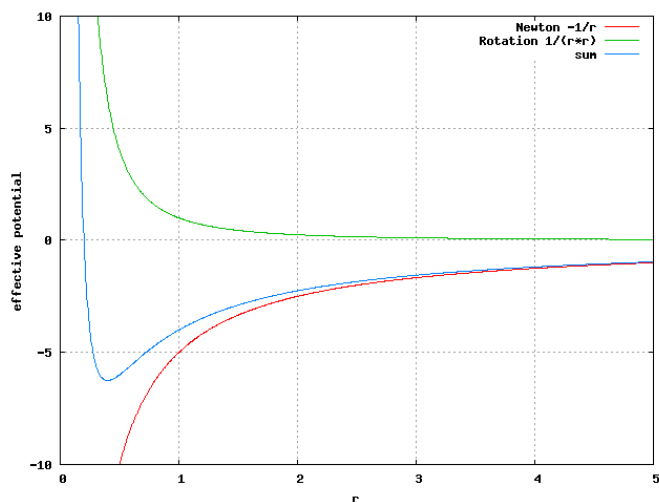


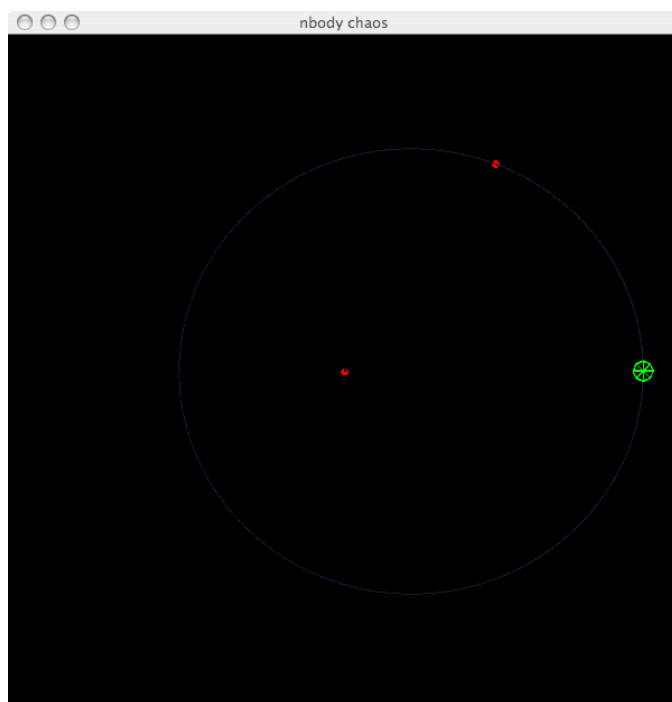Figure 1: Newtonian Potential of a point mass for a constant $l$



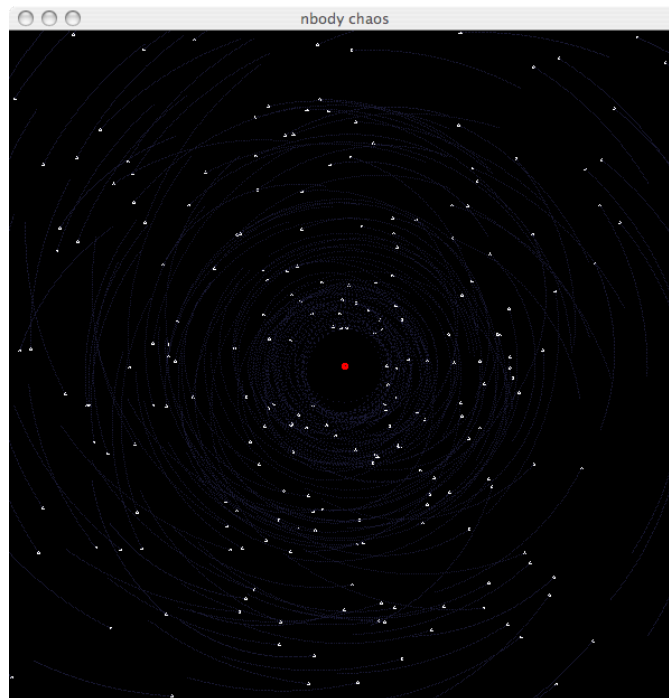Figure 2: Simulation of a test particle moving in a Newtonian Potential

Figure 3: Simulation of many test particles moving in a Newtonian Potential

## 2.2   Schwarzschild Potential

If we add the $r^{-3}$ term to the potential (21), it looks nearly the same at large scales, but it looks much different at small scales where the new term dominates. The asymptotic behavior changed from $\lim_{r \to 0} \Phi_{eff} \to \infty$ to $\lim_{r \to 0} \Phi_{eff} \to -\infty$. (See Figure 4).
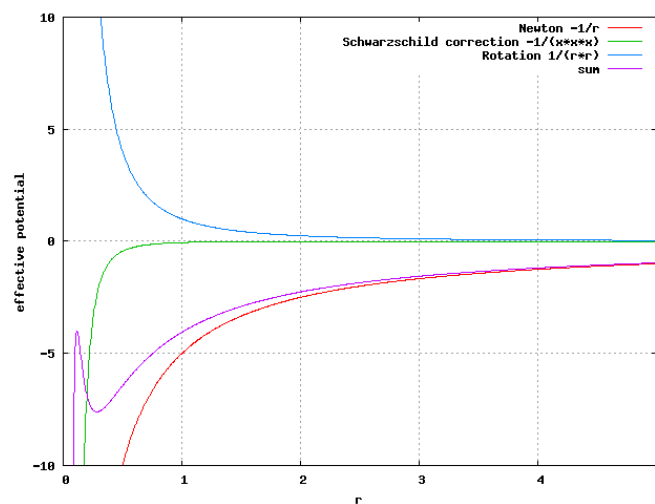


Figure 4: Schwarzschild Potential of a point mass for a constant $l$

Again, we can simulate the motion of a test particle in the new potential. The result is shown in Figure 5. You can see that the orbit isn't an ellipse anymore. The orbit's periastron gets shifted after each revolution.
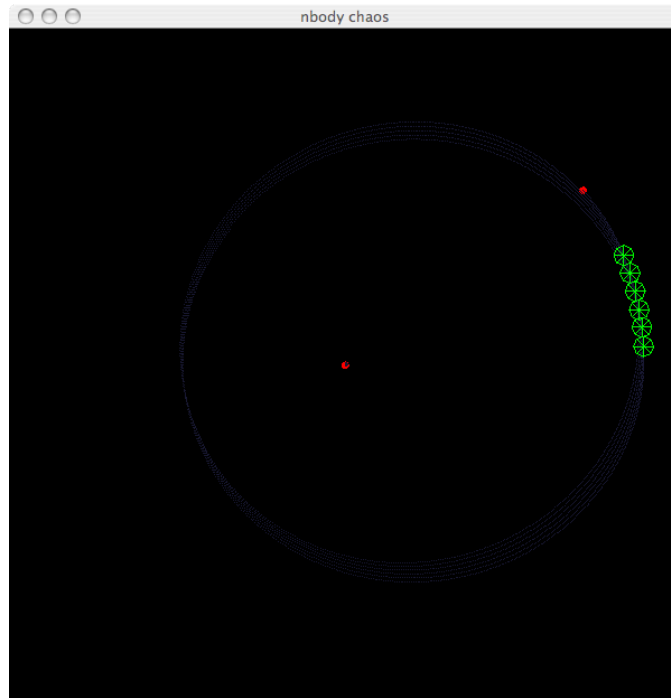
Figure 5: Simulation of a test particle moving in a Schwarzschild Potential. The aphelions of the last 6 revolutions are marked with a green circle.

We can measure the orbit of stars very close to the galactic center (see Figure 6). If there is a massive black hole, we may see this relativistic effect in the orbital motion. But the shift drawn in Figure 6 is due to the pure Newtonian effect of an extended mass distribution around the black hole (see Figure 7). This effect is much bigger than the relativistic one. However, I might be possible to detect the relativistic effect in the near future.
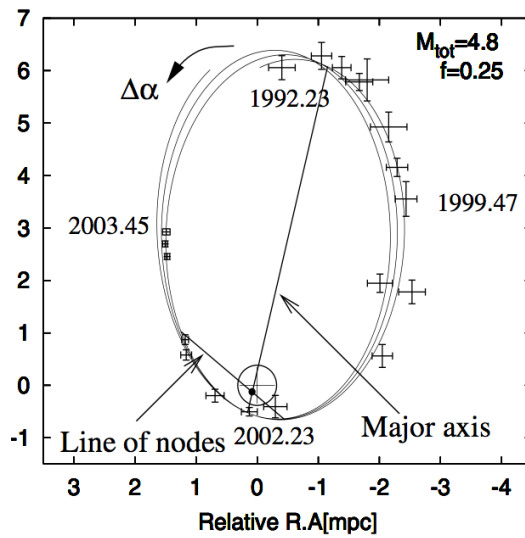


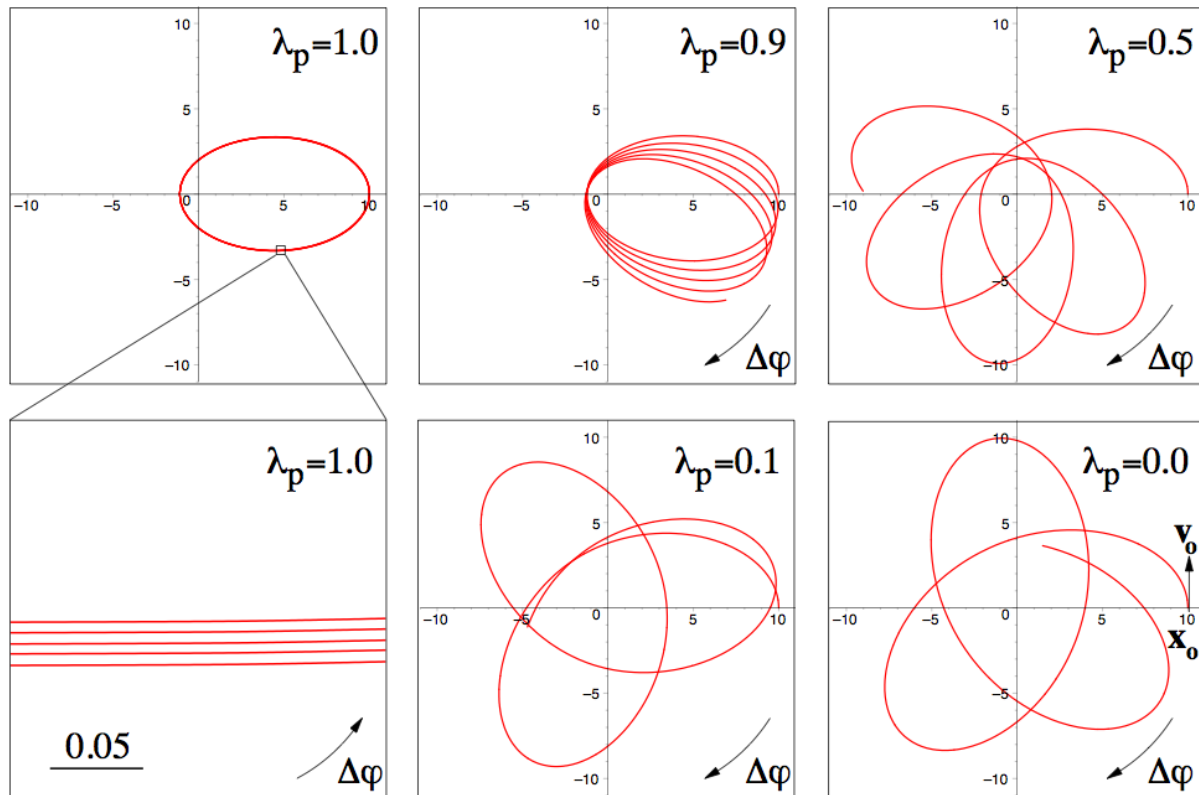Figure 6: Orbit of the star S2 around the galactic center [NM05]

Figure 7: Simulations of the S2-orbit around the galactic center [GFR01]. The parameter $\lambda_p$ corresponds to the mass fraction that is inside the back hole compared to that outside.

Another relativistic effect is the last stable orbit. In the Newtonian case, the orbit can be as small as the source is large, but this is not true in the relativistic case. As you can see in Figure 8 there exists no stable orbit anymore if $l$ is to small. The result is an area of space that is free of any orbiting particles, because every particle has either fallen into the black hole or escaped the attraction. (see Figure 9)
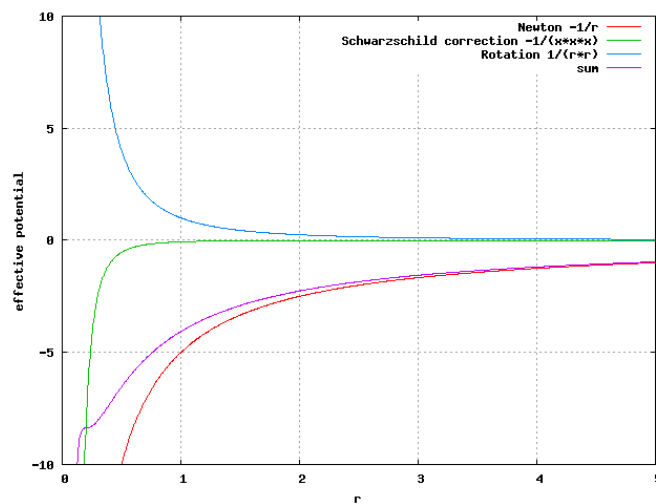


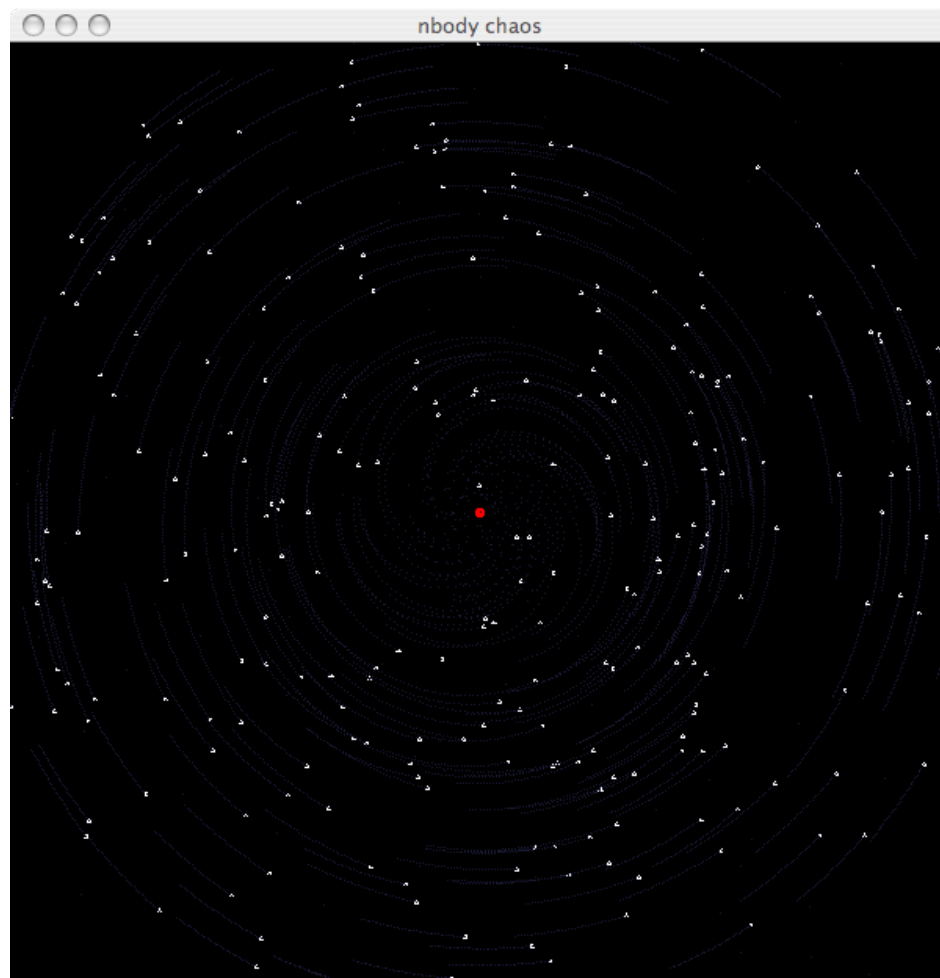Figure 8: Schwarzschild Potential of a point mass for a constant and small $l$

Figure 9: Simulation of many test particles moving in a Schwarzschild Potential. Inside some area, there is no stable orbit.

# References

[Che05]   Ta-Pei Cheng. *Relativity, Gravitation and Cosmology*. Oxford University Press, 2005.

[GFR01]  A. Eckart G. F. Rubilar. Periastron shifts of stellar orbits near the galactic center. *Astronomy and Astrophysics*, 374:94–105, 2001.

[NM05]   S. Pfalzner R. Schödel. J. Moultaka R. Spurzem N. Mouawad, A. Eckart. Weighing the cusp at the galactic centre. *Astronomische Nachrichten*, 326:83–95, 2005.